

Electromagnetic Casimir Forces in Elliptic Cylinder Geometries

Noah Graham^{1,*}

¹*Department of Physics, Middlebury College, Middlebury, VT 05753, USA*

The scattering theory approach makes it possible to carry out exact calculations of Casimir energies in any geometry for which the scattering T -matrix and a partial wave expansion of the free Green's function are available. We implement this program for the case of a perfectly conducting elliptic cylinder, thereby completing the set of geometries where electromagnetic scattering is separable. Particular emphasis is placed on the case of zero radius, where the elliptic cylinder reduces to a strip.

PACS numbers: 42.25.Fx, 03.70.+k, 12.20.-m

I. INTRODUCTION

Formulating the Casimir energy in terms of scattering theory has made it possible to efficiently reduce quantum field theory calculations to standard problems in quantum mechanics and electromagnetism. By expressing the “TGTG” form of the Casimir energy [1] in appropriate scattering bases, one can calculate the Casimir interaction energy of a collection of objects as a combination of the objects’ scattering amplitudes (T -matrices) together with universal translation matrices, which are obtained from a mode expansion of the free Green’s function [2–4]. The former are computed for each object individually, while the latter depend only on the objects’ relative positions and orientations. As a result, the Casimir energy can be computed for any collection of objects for which the scattering T -matrix is available within a standard scattering basis. This approach allows for exact calculations, extending earlier results using asymptotic expansions [5, 6] and results from scalar theories [7–9]. It can also be applied in the weak coupling approximation [10]. For objects without special symmetries, however, one must ultimately turn to computational methods to compute either the T -matrix or the associated Green’s functions [11–14].

With sufficient symmetry, the exact T -matrix can take an analytically calculable form, greatly reducing the amount of computation required. This reduction has made it possible to apply the scattering method to efficient computations of the Casimir energy for planes [15], spheres and ordinary cylinders [2, 4, 16, 17], parabolic cylinders [18, 19], and wedges and cones [20]. Here we complete the set of separable geometries in electromagnetism by treating the case of an elliptic cylinder. This geometry has been investigated for microfabricated materials using a Lifshitz formula approach in Ref. [21] and has been used to study Casimir self-energies in Refs. [22, 23].

II. SCATTERING IN ELLIPTIC CYLINDER COORDINATES

We begin by formulating scattering theory in elliptic cylinder coordinates,

$$\begin{aligned} x &= d \cosh \mu \cos \theta \\ y &= d \sinh \mu \sin \theta, \end{aligned} \tag{1}$$

where $2d$ is the interfocal separation of our elliptic cylinder coordinates, θ is the analog of the angle in ordinary cylindrical coordinates, and μ is the analog of the radius, with

$$r = \sqrt{x^2 + y^2} = d \sqrt{\frac{\cosh 2\mu + \cos 2\theta}{2}} \rightarrow \frac{d}{2} e^\mu \tag{2}$$

as $\mu \rightarrow \infty$.

We use separation of variables to form solutions of the Helmholtz equation $-\nabla^2 \psi(\mathbf{r}) = k^2 \psi(\mathbf{r})$ as products of functions of μ , θ and z individually. For the functions of z , we have ordinary complex exponentials $e^{ik_z z}$, which will multiply angular functions of θ and radial functions of μ . Since we have parity symmetry, we can choose our angular solutions to be either even or odd under reflection across the x -axis, $\theta \rightarrow -\theta$. Unlike the ordinary cylinder case, the

*Electronic address: ngraham@middlebury.edu

elliptic angular solutions depend on the wave number k , and the elliptic radial solutions associated with the odd and even angular solutions differ and depend on the wave number and radius separately, rather than only on the product kr . For $q = \frac{d^2}{4}(k^2 - k_z^2)$, the angular solutions are the even and odd angular Mathieu functions $ce_m(\theta, q)$ and $se_m(\theta, q)$, which are the analogs of $\cos m\theta$ and $\sin m\theta$ respectively. As in the case of ordinary cylindrical coordinates, for the even functions m runs from 0 to ∞ , while for the odd functions m runs from 1 to ∞ . For the corresponding radial functions, we have both the even and odd first kind solutions $Je_m(\mu, q)$ and $Jo_m(\mu, q)$, the analogs of the Bessel function $J_m(\sqrt{k^2 - k_z^2}r)$, and the even and odd outgoing wave solutions $He_m(\mu, q)$ and $Ho_m(\mu, q)$, the analogs of the Hankel function $H_m^{(1)}(\sqrt{k^2 - k_z^2}r)$. We will normalize the Mathieu functions so that they obey the same orthonormality conditions as their cylindrical analogs, except that the $m = 0$ even angular function will be normalized so that its root mean square average value is $1/\sqrt{2}$ (the same as for all the other angular functions) instead of $\cos 0 = 1$. As a result, we have

$$\int_0^{2\pi} ce_m(\theta, q)^2 d\theta = \int_0^{2\pi} se_m(\theta, q)^2 d\theta = \pi, \quad (3)$$

with the radial functions normalized to coincide with their cylindrical analogs asymptotically. Our notation and normalization match that of Ref. [24], which defines Mathieu functions following the conventions of Abramowitz and Stegun [25], but uses a modified notation that is more closely analogous to the ordinary cylinder case. We will make use of identities for elliptic cylinder functions found in standard references [25–27].

The key ingredients for our calculation will be the free Green's function

$$G(\mathbf{r}_1, \mathbf{r}_2, k) = \int_{-\infty}^{\infty} \frac{dk_z}{2\pi} \frac{i}{2} \left[\sum_{m=0}^{\infty} ce_m(\theta_1, q) ce_m(\theta_2, q) Je_m(\mu_{<}, q) He_m(\mu_{>}, q) + \sum_{m=1}^{\infty} se_m(\theta_1, q) se_m(\theta_2, q) Jo_m(\mu_{<}, q) Ho_m(\mu_{>}, q) \right], \quad (4)$$

where $\mu_{<} (\mu_{>})$ is the smaller (larger) of μ_1 and μ_2 , and the expansion of a plane wave,

$$e^{i\mathbf{k}\cdot\mathbf{r}} = e^{ik_z z} \left[2 \sum_{m=0}^{\infty} i^m ce_m(\phi, q) ce_m(\theta, q) Je_m(\mu, q) + 2 \sum_{m=1}^{\infty} i^m se_m(\phi, q) se_m(\theta, q) Jo_m(\mu, q) \right], \quad (5)$$

where μ , θ , and z are the elliptic cylinder coordinates of \mathbf{r} and $\phi = \arctan \frac{k_y}{k_x}$ is the angle of $\mathbf{k} = (k_x, k_y, k_z)$ in the xy -plane, with $k^2 = k_x^2 + k_y^2 + k_z^2$.

We will work on the imaginary k -axis $k = i\kappa$, so that $k_y = i\sqrt{\kappa^2 + k_x^2 + k_z^2}$ and $q = -d^2(\kappa^2 + k_z^2)/4$ is negative. As a result, it is convenient to rewrite these expressions in terms of modified radial functions,

$$G(\mathbf{r}_1, \mathbf{r}_2, k) = \int_{-\infty}^{\infty} \frac{dk_z}{2\pi} \frac{1}{\pi} \left[\sum_{m=0}^{\infty} ce_m(\theta_1, q) ce_m(\theta_2, q) Ie_m(\mu_{<}, -q) Ke_m(\mu_{>}, -q) + \sum_{m=1}^{\infty} se_m(\theta_1, q) se_m(\theta_2, q) Io_m(\mu_{<}, -q) Ko_m(\mu_{>}, -q) \right] \quad (6)$$

and

$$e^{i\mathbf{k}\cdot\mathbf{r}} = e^{ik_z z} \left[2 \sum_{m=0}^{\infty} (-1)^m ce_m(\phi, q) ce_m(\theta, q) Ie_m(\mu, -q) + 2 \sum_{m=1}^{\infty} (-1)^m se_m(\phi, q) se_m(\theta, q) Io_m(\mu, -q) \right], \quad (7)$$

where $Ie_m(\mu, -q) = i^{-m} Je_m(\mu, q)$, $Io_m(\mu, -q) = i^{-m} Jo_m(\mu, q)$, $Ke_m(\mu, -q) = i^{m+1} \frac{\pi}{2} He_m(\mu, q)$ and $Ko_m(\mu, -q) = i^{m+1} \frac{\pi}{2} Ho_m(\mu, q)$ are the modified outgoing radial functions.

We will consider scattering with Dirichlet and Neumann boundary conditions on an elliptic cylinder of radius μ_0 . For the scattering amplitudes, we have $\mathcal{T}_{mk_z m' k'_z}^{e,o} = 2\pi \delta(k_z - k'_z) \delta_{mm'} \mathcal{T}_m^{e,o}$, with

$$\begin{aligned} \mathcal{T}_m^e &= -\frac{Ie_m(\mu_0, -q)}{Ke_m(\mu_0, -q)} & \mathcal{T}_m^o &= -\frac{Io_m(\mu_0, -q)}{Ko_m(\mu_0, -q)} & (\text{Dirichlet}) \\ \mathcal{T}_m^e &= -\frac{Ie'_m(\mu_0, -q)}{Ke'_m(\mu_0, -q)} & \mathcal{T}_m^o &= -\frac{Io'_m(\mu_0, -q)}{Ko'_m(\mu_0, -q)} & (\text{Neumann}), \end{aligned} \quad (8)$$

where prime indicates a derivative with respect to μ .

III. ELLIPTIC CYLINDER AND PLANE

To consider the elliptic cylinder's interaction with a plane, we will need to connect the elliptic cylinder and planar geometries. To do so, we make use of the expression for the free Green's function in Cartesian coordinates for $y_2 > y_1$,

$$G(\mathbf{r}_1, \mathbf{r}_2, k) = \int_{-\infty}^{\infty} \frac{dk_z}{2\pi} e^{ik_z(z_2 - z_1)} \frac{i}{4\pi} \int_{-\infty}^{\infty} \frac{dk_x}{k_y} e^{i(k_x(x_2 - x_1) + k_y(y_2 - y_1))}, \quad (9)$$

where $k_y = \sqrt{k^2 - k_x^2 - k_z^2} = i\sqrt{\kappa^2 + k_x^2 + k_z^2}$. We equate Eq. (9) to the Green's function in Eq. (6), expand the plane wave $e^{i\mathbf{k} \cdot \mathbf{r}_2}$ in Eq. (9) using Eq. (7), make the substitution $k_x \rightarrow -k_x$, and finally use the orthogonality of the regular elliptic cylinder solutions to equate both sides term by term in the sums over m . The result is an expansion for the elliptic outgoing wave solutions in terms of plane waves for $y < 0$ [25],

$$\begin{aligned} ce_m(\theta, q)Ke_m(\mu, -q)e^{ik_z z} &= \int_{-\infty}^{\infty} dk_x \left[\frac{i}{2k_y} ce_m(\phi, q) \right] e^{-ik_y y + ik_x x} e^{ik_z z} \\ se_m(\theta, q)Ko_m(\mu, -q)e^{ik_z z} &= \int_{-\infty}^{\infty} dk_x \left[\frac{-i}{2k_y} se_m(\phi, q) \right] e^{-ik_y y + ik_x x} e^{ik_z z}. \end{aligned} \quad (10)$$

The quantities in brackets represent the translation matrix elements, which we must then multiply by the normalization factor $\frac{C_m^{\text{elliptic}}}{C_{k_x}^{\text{plane}}}$, where we can read off $C_m^{\text{elliptic}} = \sqrt{\frac{1}{\pi}}$ and $C_{k_x}^{\text{plane}} = \sqrt{\frac{i}{4\pi k_y}}$ from the expressions for the free Green's function in Eqs. (6) and (9).

Finally, the T -matrix elements for the plane in Cartesian coordinates are simply $\mathcal{T}^P = \pm 1$ for Neumann and Dirichlet boundary conditions respectively. (For more general boundary conditions on the plane, this scattering amplitude would be a function of k_x .)

We have now obtained the T -matrix elements, which describe how waves scatter off each object individually, and the translation matrix elements, which convert the scattering bases between the two objects. As a result, we are prepared to assemble these ingredients into the result for the full Casimir interaction energy per unit length. We consider a perfectly conducting plane oriented perpendicular to the y -axis and a perfectly conducting elliptic cylinder with its z -axis parallel to the plane, its center at a distance H from the plane, and its major axis at an angle φ to the plane, as shown in Fig. 1. This angle represents a rotation of the elliptic cylinder coordinates θ and μ relative to the Cartesian coordinates x and y , which we then implement in Eq. (10) by adding a constant shift φ to the angle $\phi = \arctan \frac{k_y}{k_x}$ in the translation matrix elements.

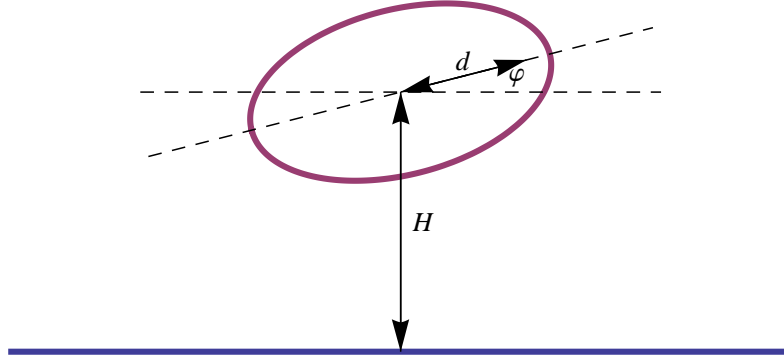


FIG. 1: Geometry for the elliptic cylinder and plane.

For a particular choice of boundary conditions, we can now use the approach of Refs. [2–4] to write the Casimir energy per unit length as

$$\frac{\mathcal{E}}{\hbar c L} = \int_0^\infty \frac{d\kappa}{2\pi} \int_{-\infty}^\infty \frac{dk_z}{2\pi} \log \det \left(\mathbb{1}_{mm'}^{\chi\chi'} - \mathcal{T}_m^\chi \int \frac{idk_x}{k_y} \mathcal{U}_{mk_x}^\chi \mathcal{T}_{k_x}^P \hat{\mathcal{U}}_{m'k_x}^{\chi'} \right), \quad (11)$$

where the matrix determinant runs over $\chi, \chi' = o, e$ with $m = 0, 1, 2, 3 \dots$ for $\chi = e$ and $m = 1, 2, 3 \dots$ for $\chi = o$, and similarly for m' and χ' . The translation matrices $\mathcal{U}_{mk_x}^\chi$ and reverse translation matrices $\hat{\mathcal{U}}_{mk_x}^\chi$ are given by

$$\mathcal{U}_{mk_x}^e = ce_m(\phi + \varphi, q) e^{ik_y H} \quad \hat{\mathcal{U}}_{mk_x}^e = ce_m(-\phi + \varphi, q) e^{ik_y H} \quad (12)$$

for the even modes and

$$\mathcal{U}_{mk_x}^o = se_m(\phi + \varphi, q) e^{ik_y H} \quad \hat{\mathcal{U}}_{mk_x}^o = se_m(-\phi + \varphi, q) e^{ik_y H} \quad (13)$$

for the odd modes.

We can then change the integration variable from k_x to $u = \frac{1}{i}(\phi - \frac{\pi}{2})$ and combine the κ and k_z equations into a single integral over $p = \sqrt{\kappa^2 + k_z^2}$, so that $q = -\frac{d^2 p^2}{4}$. We obtain

$$\frac{\mathcal{E}}{\hbar c L} = \frac{1}{4\pi} \int_0^\infty p dp \log \det \left[\mathbb{1}_{mm'}^{\chi\chi'} - \mathcal{T}_m^\chi \mathcal{T}^P \int_{-\infty}^\infty du e^{-2pH \cosh u} \frac{ce_m}{se_m} \left(\frac{\pi}{2} + iu + \varphi, q \right) \frac{ce_{m'}}{se_{m'}} \left(\frac{\pi}{2} - iu + \varphi, q \right) \right], \quad (14)$$

where we choose ce_m for $\chi = e$ and se_m for $\chi = o$, and similarly for m' and χ' . The full electromagnetic Casimir energy is the sum of this result for Dirichlet conditions on both surfaces and for Neumann conditions on both surfaces. Note that the established result for an ordinary cylinder [16] can be obtained from this expression by replacing the elliptic functions with their ordinary cylindrical analogs, combining the even and odd modes using $\cosh mu \cosh m'u + \sinh mu \sinh m'u = \cosh(m + m')u$, and employing the integral identity

$$K_n(\sigma) = \int_0^\infty e^{-\sigma \cosh u} \cosh nu \, du. \quad (15)$$

There are several special cases of interest in which the calculation simplifies:

- Plane perpendicular to the ellipse's major axis.

For $\varphi = \pi/2$, the elliptic cylinder's major axis runs perpendicular to the plane. By the reflection symmetry across the y -axis, the even and odd sectors decouple, and we can compute the Casimir energy by considering the odd and even elliptic modes separately.

- Plane parallel to the ellipse's major axis.

For $\varphi = 0$, the elliptic cylinder's major axis lies parallel to the plane. This case also has reflection symmetry across the y -axis, but this symmetry does not correspond directly to the symmetry of the even and odd Mathieu functions. Instead, the even Mathieu functions of even order and the odd Mathieu functions of odd order are symmetric under this transformation, while the odd Mathieu functions of even order and the even Mathieu functions of odd order are antisymmetric. (This is the same symmetry structure as the ordinary trigonometric functions have when their argument is displaced by $\pi/2$.) Thus we can again decompose the problem into two independent sectors, consisting of the modes for which the parity of the elliptic functions matches the parity of m , and the modes for which they are opposite.

- Zero radius cylinder.

An elliptic cylinder with $\mu_0 = 0$ becomes a strip of width $2d$, allowing us to study the effects of edges [18–20, 28, 29]. In that case we have $\mathcal{T}_m^o = 0$ for a Dirichlet boundary and $\mathcal{T}_m^e = 0$ for a Neumann boundary, since in these cases the free modes already obey the boundary condition at the surface. These modes therefore give zero contribution to the Casimir energy in this case, and can be omitted from the calculation.

IV. NUMERICAL RESULTS

We can now compute the Casimir energy by straightforward numerical integration of Eq. (14). To compute the modified radial functions needed for the scattering amplitude, we use the package of Alhargan [30, 31]. (Standard packages such as Maple and Mathematica only implement the angular Mathieu functions of the first kind. Although the radial functions are related to the angular functions with imaginary argument, without an implementation of the second kind angular function we cannot take advantage of this relationship to compute the functions needed to for the scattering amplitude.) The angular functions arising from the translation matrix, on the other hand, need to be computed for complex arguments, which are not supported directly in the Alhargan package. Fortunately, since only the first kind angular functions are required, we can use the implementation in Mathematica, which supports fully complex arguments. As a final complication, because of problems with the Mathieu function routines in the current version of Mathematica for the case where the parameter $q < 0$, we make use of the identities

$$ce_m(\mu, q) = \begin{cases} (-1)^{\frac{m}{2}} ce_m\left(\frac{\pi}{2} - \mu, -q\right) & \text{for } m \text{ even} \\ (-1)^{\frac{m-1}{2}} se_m\left(\frac{\pi}{2} - \mu, -q\right) & \text{for } m \text{ odd} \end{cases}$$

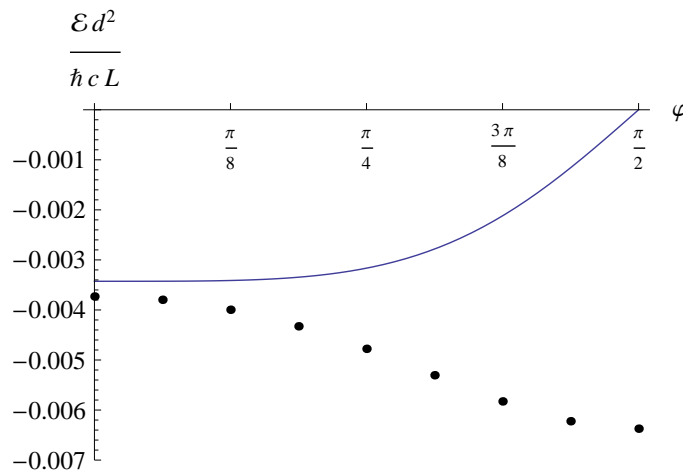


FIG. 2: Electromagnetic Casimir interaction energy for a perfectly conducting strip opposite a perfectly conducting plane, as a function of the orientation angle φ . The distance H from the center of the strip to the plane is twice the distance from the center of the strip to the edge of the strip, $H = 2d$. The solid line shows the proximity force approximation.

$$se_m(\mu, q) = \begin{cases} (-1)^{\frac{m}{2}-1} se_m\left(\frac{\pi}{2} - \mu, -q\right) & \text{for } m \text{ even} \\ (-1)^{\frac{m-1}{2}} ce_m\left(\frac{\pi}{2} - \mu, -q\right) & \text{for } m \text{ odd} \end{cases} \quad (16)$$

so that we only need to compute the angular functions for $-q > 0$. As a result, after importing the Alhargan routines for the modified radial functions, it is possible to carry out the full calculation within Mathematica. Because of limitations in the ability of the angular routines to handle large imaginary arguments, however, it was not possible to extend the calculation to very small separations.

Figure 2 shows the orientation dependence of the Casimir interaction energy for a perfectly conducting strip (an elliptic cylinder of zero radius) for the case where the distance H from the center of the strip to the plane is twice the distance from the center of the strip to the edge of the strip, $H = 2d$. Because higher values did not change the results appreciably, the matrix determinants were truncated at $m_{\max} = 8$. We see that the lowest energy occurs for $\varphi = \pi/2$, when the strip is perpendicular to the plane. As expected, the result for the energy per unit length in this case, $\frac{\mathcal{E}d^2}{\hbar c L} = -0.00637$, is less negative than the -0.00674 one finds [18, 19] for the case where the strip is extended to an infinite half-plane whose edge maintains the same distance $H - d = d$ from the infinite plane. We note, however, that if we subtract the contribution from a half-plane at distance $H + d = 3d$ from the result for the half-plane at distance $H - d = d$ to account for the missing remainder of the half plane, we obtain $-0.00674 \cdot \frac{8}{9} = -0.00599$, which underestimates the magnitude of the true result for the strip. We also compare these results to the proximity force approximation (PFA),

$$\frac{\mathcal{E}_{PFA}^{(0)}}{\hbar c L} = -\frac{\pi^2}{720} \int_{-d \cos \varphi}^{-d \cos \varphi} \frac{dx}{(H + x \tan \varphi)^3} = -\frac{\pi^2}{360} \frac{H d \cos \varphi}{(H^2 - d^2 \sin^2 \varphi)^2} \quad (17)$$

which gives a good approximation for $\varphi = 0$ but goes to zero at $\varphi = \pi/2$. For $\varphi \neq 0$ the derivative expansion correction to the PFA [32, 33] is also invalid, because of the sharp curvature at the point of closest approach.

Figure 3 shows the Casimir interaction energy for a strip oriented parallel to a plane as a function of the distance to the plane. The energy is shown as a ratio with the PFA result (in this case the correction from the derivative expansion vanishes). As in the case of the ordinary cylinder [16], the PFA is an underestimate at large distances, but at short distances the exact result approaches the PFA result from below. These calculations were carried out with the matrices truncated at several different values of m_{\max} up to $m_{\max} = 16$, with the final result then obtained by extrapolating these results for $m_{\max} \rightarrow \infty$.

V. DISCUSSION

We have computed the Casimir interaction energy for an elliptic cylinder, the last remaining geometry for which electromagnetic scattering is separable. For a plane, cylinder, and sphere, the problem remains separable even for a dielectric, while for a parabolic cylinder, elliptic cylinder, wedge, and cone only perfect conductors can be solved

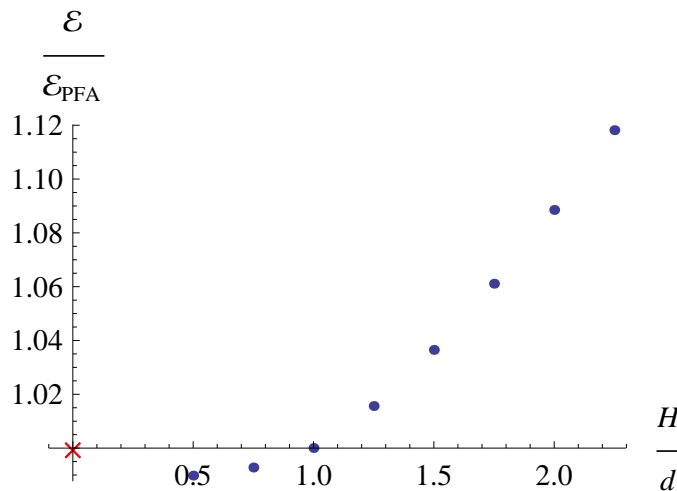


FIG. 3: Ratio of the electromagnetic Casimir interaction energy to the proximity force approximation (PFA) for a perfectly conducting strip of width $2d$ parallel to a perfectly conducting plane, as a function of the separation H . As in the case of an ordinary cylinder [16], the ratio is a nonmonotonic function of H .

exactly. However, the scattering method is particularly useful in these latter cases, because they contain sharp limits in which the PFA is invalid. In principle, it should be possible to extend the elliptic cylinder result to a hyperbolic cylinder in the same way as the wedge is obtained from the ordinary cylinder and the cone is obtained from the sphere, but at present there do not appear to be routines available for computing all the Mathieu functions of complex order that would be needed for such a calculation.

Focusing on the limit in which the elliptic cylinder becomes a strip has made it possible to study the orientation dependence of the Casimir force, to show how the PFA depends on distance and angle, and to observe non-superposition effects in the perpendicular configuration (where the PFA is invalid). With improvements to the available routines for computing Mathieu functions, this calculation could offer an independent check of the edge correction that was obtained for half-planes [18, 19, 34]. More generally, this calculation establishes another addition to the toolbox of Casimir problems that can be cast into analytically tractable form.

VI. ACKNOWLEDGEMENTS

N. G. thanks T. Emig, R. L. Jaffe, M. Kardar, and K. Milton for helpful conversations and suggestions. This work was supported in part by the National Science Foundation (NSF) through grant PHY-1213456.

-
- [1] O. Kenneth and I. Klich, Phys. Rev. Lett. **97**, 160401 (2006).
 - [2] T. Emig, N. Graham, R. L. Jaffe, and M. Kardar, Phys. Rev. Lett. **99**, 170403 (2007).
 - [3] T. Emig, N. Graham, R. L. Jaffe, and M. Kardar, Phys. Rev. **D77**, 025005 (2008).
 - [4] S. J. Rahi, T. Emig, N. Graham, R. L. Jaffe, and M. Kardar, Phys. Rev. **D80**, 085021 (2009).
 - [5] R. Balian and B. Duplantier, Annals Phys. **104**, 300 (1977).
 - [6] R. Balian and B. Duplantier, Annals Phys. **112**, 165 (1978).
 - [7] A. Bulgac and A. Wirzba, Phys. Rev. Lett. **87**, 120404 (2001).
 - [8] A. Bulgac, P. Magierski, and A. Wirzba, Phys. Rev. **D73**, 025007 (2006).
 - [9] A. Wirzba, J. Phys. **A41**, 164003 (2008).
 - [10] K. A. Milton and J. Wagner, Phys. Rev. **D77**, 045005 (2008).
 - [11] M. T. H. Reid, A. W. Rodriguez, J. White, and S. G. Johnson, Phys. Rev. Lett. **103**, 040401 (2009).
 - [12] H. Gies, K. Langfeld, and L. Moyaerts, JHEP **0306**, 018 (2003).
 - [13] H. Gies and K. Klingmuller, Phys. Rev. **D74**, 045002 (2006).
 - [14] A. Forrow and N. Graham, Phys. Rev. **A86**, 062715 (2012).
 - [15] A. Lambrecht, P. A. Maia Neto, and S. Reynaud, New J. Phys. **8**, 243 (2006).
 - [16] T. Emig, R. L. Jaffe, M. Kardar, and A. Scardicchio, Phys. Rev. Lett. **96**, 080403 (2006).
 - [17] L. P. Teo, Phys. Rev. **D87**, 045021 (2012).

- [18] N. Graham, A. Shpunt, T. Emig, S. J. Rahi, R. L. Jaffe, and M. Kardar, Phys. Rev. **D81**, 061701 (2010).
- [19] N. Graham, A. Shpunt, T. Emig, S. J. Rahi, R. L. Jaffe, and M. Kardar, Phys. Rev. **D83**, 125007 (2011).
- [20] M. F. Maghrebi, S. J. Rahi, T. Emig, N. Graham, R. L. Jaffe, and M. Kardar, Proc. Nat. Acad. Sci. **108**, 6867 (2011).
- [21] R. S. Decca, E. Fischbach, G. L. Klimchitskaya, D. E. Krause, D. López, and V. M. Mostepanenko, Phys. Rev. **A84**, 042502 (2011).
- [22] A. R. Kitson and A. Romeo, Phys.Rev. **D74**, 085024 (2006).
- [23] J. P. Straley, G. A. White, and E. B. Kolomeisky, Phys. Rev. **A87**, 022503 (2013).
- [24] N. Graham and K. D. Olum, Phys. Rev. **D72**, 025013 (2005).
- [25] M. Abramowitz and I. A. Stegun, *Handbook of Mathematical Functions With Formulas, Graphs, and Mathematical Tables* (U.S. government printing office, Washington, 1972).
- [26] P. M. Morse and H. Feshbach, *Methods of Theoretical Physics* (McGraw-Hill, New York, 1953).
- [27] Bateman manuscript project, *Higher transcendental functions*, vol. 1 (McGraw-Hill, New York, 1953).
- [28] H. Gies and K. Klingmuller, Phys. Rev. Lett. **97**, 220405 (2006).
- [29] D. Kabat, D. Karabali, and V. Nair, Phys. Rev. **D81**, 125013 (2010).
- [30] F. Alhargan, ACM T Math Software **26**, 390 (2000).
- [31] F. Alhargan, ACM T Math Software **26**, 408 (2000).
- [32] C. D. Fosco, F. C. Lombardo, and F. D. Mazzitelli, Phys. Rev. **D84**, 105031 (2011).
- [33] G. Bimonte, T. Emig, R. L. Jaffe, and M. Kardar, Europhysics Letters **97**, 50001 (2012).
- [34] M. F. Maghrebi and N. Graham, Europhys. Lett. **95**, 14001 (2011).